Vacuum phase transition solves the H_0 tension

Eleonora Di Valentino,[1,*] Eric V. Linder,[2,3,†] and Alessandro Melchiorri[4,‡]

[1]*Jodrell Bank Center for Astrophysics, School of Physics and Astronomy, University of Manchester,
Oxford Road, Manchester M13 9PL, United Kingdom*
[2]*Berkeley Center for Cosmological Physics & Berkeley Lab, University of California,
Berkeley, California 94720, USA*
[3]*Energetic Cosmos Laboratory, Nazarbayev University, Astana 010000, Kazakhstan*
[4]*Physics Department and INFN, Università di Roma "La Sapienza," Ple Aldo Moro 2, 00185 Rome, Italy*

Taking the Planck cosmic microwave background data and the more direct Hubble constant measurement data as unaffected by systematic offsets, the values of the Hubble constant H_0 interpreted within the ΛCDM cosmological constant and cold dark matter cosmological model are in $\sim 3.3\sigma$ tension. We show that the Parker vacuum metamorphosis (VM) model, physically motivated by quantum gravitational effects and with the same number of parameters as ΛCDM, can remove the H_0 tension and can give an improved fit to data (up to a mean $\Delta\chi^2 = -7.5$). It also ameliorates tensions with weak lensing data and the high redshift Lyman alpha forest data. Considering Bayesian evidence, we found in the case of the Planck data set alone positive evidence for a VM model against a cosmological constant both in the six- and nine-parameter framework. When the R16 data set is also considered, we found a strong evidence for the VM model against a cosmological constant in nine-parameter space. We separately consider a scale-dependent scaling of the gravitational lensing amplitude, such as provided by modified gravity, neutrino mass, or cold dark energy, motivated by the somewhat different cosmological parameter estimates for low and high CMB multipoles. We find that no such scale dependence is preferred.

I. INTRODUCTION

Cosmic microwave background (CMB) measurements provide highly precise probes of the conditions and energy components of the Universe over the entire age of the Universe. Moreover, they can reveal the total age and scale of the Universe, and so the present Hubble constant H_0. The Hubble constant can also be determined through local distance measurements, e.g. through cross-calibration of Cepheid and type Ia supernova distances [1,2]. The latest values from these two methods, within the concordance ΛCDM model with a cosmological constant plus cold dark matter, are in $\sim 3\sigma$ tension. This is probably the most relevant tension present between current cosmological data sets, and several works have recently appeared discussing it or proposing different theoretical mechanisms as solution (see e.g. [3–17]).

Taking each set of cosmological data at face value (cf. [18–21] regarding local H_0), we found in [22] that the H_0 values could be consistent in a parameter space expanded to include further, not unreasonable, cosmological physics. In particular, altering the mechanism for cosmic acceleration from a cosmological constant to a particular form of dynamical dark energy would remove the tension. However, the form of dark energy required was quite unusual, not corresponding to the usual scalar field dark energy models. It needed to be phantom, with equation of state parameter $w < -1$, and, moreover, be rapidly evolving.

These properties generally are not held simultaneously since they tend to exacerbate problems of fine-tuning and stability. However, there is a model considered in the early days of dark energy investigations that possesses just these phenomenological properties, from a sound theoretical foundation: the vacuum metamorphosis (VM) model of [23–25], which has a phase transition in the nature of the vacuum. In this article, we explore the observational viability of VM in fitting the data simultaneously and removing the tension in H_0 values.

Another peculiarity in the data is that cosmological parameters estimated from small scales (CMB multipoles $\ell \gtrsim 1000$) are somewhat offset relative to the values estimated from large scales ($\ell \lesssim 1000$) [26–29]. In particular, larger scales show some preference for a higher Hubble constant. We, therefore, separately explore cosmology fitting in a ΛCDM parameter space extended to allow for a scale-dependent CMB lensing parameter A_{lens}, reflecting some (unspecified) nonstandard scale-dependent physics.

*eleonora.divalentino@manchester.ac.uk
†evlinder@lbl.gov
‡alessandro.melchiorri@roma1.infn.it

043528-1

Section II introduces the VM model and lays out the foundation for using it with CMB and distance data. In Sec. III, we present the cosmology fitting data and procedure. We carry out Markov chain Monte Carlo (MCMC) fits to the data for the VM model in Sec. IV in the baseline and the extended parameter spaces and discuss the results. In Sec. V, we investigate an alternative approach to addressing the tension through the use of a scale-dependent A_{lens}. We conclude in Sec. VI.

II. VACUUM METAMORPHOSIS

A. Background

The two main data sets in tension on the value of H_0 are the CMB data from the Planck satellite [30] and the distance measurements from [2], hereafter called R16. Taking the Planck + R16 constraints in the w_0–w_a plane at face value, [31] found that they prefer the phantom region $w < -1$ and more deeply phantom in the past ($w_a < 0$, [22]). A single canonical scalar field cannot achieve this, and even more complicated, and effectively arbitrary, fields have difficulty. While adding the JLA supernova constraints [32] tends to shift the preferred area out of the phantom region, and adding baryon acoustic oscillation (BAO) data [33–35] tends to prefer less negative values of w_a, adding weak lensing or CMB lensing preserves the preference for deep phantom models. Here we mostly focus on just the Planck or Planck + R16 data sets.

It is interesting to consider whether a reasonably physically motivated model can be found for this unusual region. The answer is yes: one of the earliest dark energy models, vacuum metamorphosis [23–25] lives in just this part of phase space. This model has a sound physical foundation, taking into account quantum loop corrections to gravity in the presence of a massive scalar field. In the first order calculations, this gives rise to R^2 terms familiar from, e.g., Starobinsky gravity and inflation [36], where R is the Ricci scalar, but Parker and collaborators were able to nonperturbatively sum the infinite series (under certain restrictions) and find a closed form solution.

This solution indicates a phase transition in gravity similar to Sakharov's induced gravity [37]. The phase transition is induced once the Ricci scalar curvature R has evolved to become of order the mass squared of the field, and thereafter R is frozen to be of order m^2. This original model had one free parameter, m^2, which determined the matter density today, Ω_m, giving it the same number of free parameters as flat ΛCDM.

Some later elaborations added a vacuum expectation value, somewhat inorganically, acting as a cosmological constant, but we will focus on the original, more elegant VM model.

B. Relation to w_0–w_a

A first question might be how to connect the observational motivation for a particular region in the dark energy

equation of state phase space w_0–w_a, where w_0 is the present value of the equation of state function $w(a)$ and w_a a measure of its time variation, to the theoretical VM model. It has been well established that the w_0–w_a parametrization provides an excellent fit (at the 0.1% level in observables) to a broad range of scalar field models [38,39], but VM has a very rapid time evolution and is not a standard scalar field model.

In Fig. 1, we illustrate the equation of state behavior for the original, and some elaborated, VM models. One clearly sees the phase transition at a fairly recent redshift, where the dark energy deviates from an effective cosmological constant behavior of $w = -1$ (for the elaborated cases) or newly appears in the phase transition (in the original case). After the transition the dark energy is highly phantom ($w < -1$) and then rapidly evolves toward $w = -1$ (with w_a strongly negative) and an eventual de Sitter state as the Ricci scalar freezes to the value of the field mass squared.

Even for the rapidly evolving case of no cosmological constant (our preferred case), the observational implications of the model are well described by the standard w_0–w_a parametrization since the phantom nature means that dark energy diminishes quickly into the past. Figure 2 illustrates the goodness of fit of the equivalent w_0–w_a model for the most extreme case, that without a cosmological constant. The agreement in the distance-redshift relation is better
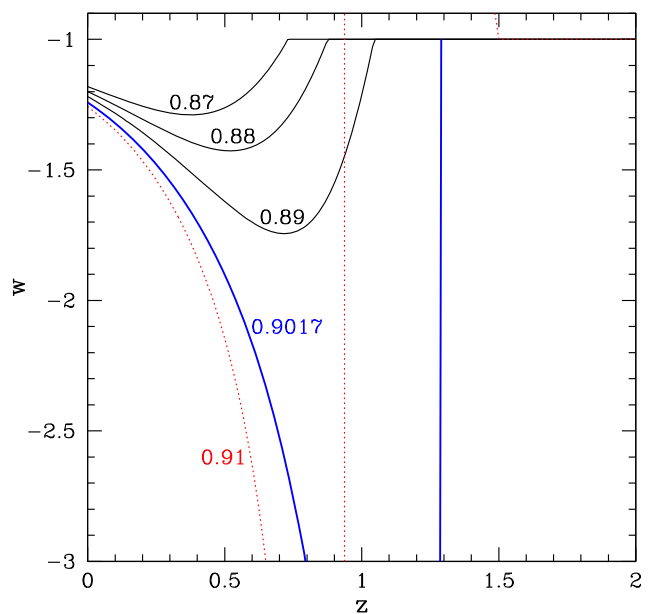

FIG. 1. The effective dark energy equation of state evolution is plotted vs redshift for several values of the mass parameter M, for $\Omega_m = 0.3$. The bold blue curve shows the original case (our preferred model) where there is no cosmological constant, while the medium black curves show the elaborated case with an added cosmological constant, and the dotted red curve shows one with a negative cosmological constant (causing w to first shoot up to large positive values before it plummets to highly negative values).
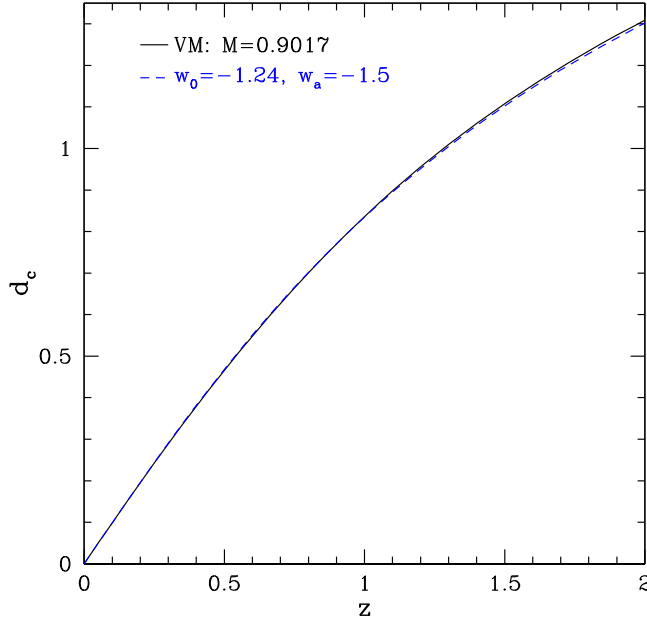
FIG. 2. The distance-redshift relation for the vacuum meta-morphosis model without a cosmological constant—the fastest evolving one—is well fit by a standard w_0–w_a model. Here, the comoving distance, which enters the CMB distance to last scattering, and weak lensing, BAO, and supernova observations, is plotted vs redshift.

than 0.55% at all redshifts (0.2% in the distance to CMB last scattering), sufficient for current data precision. Note that $w_0 = -1.24$, $w_a = -1.5$ is a good fit (lying near 68% C.L.) to the Planck + R16 data, as well as when adding weak lensing or CMB lensing or shifting the local distance H_0 prior not lower than 70, as seen in [22].

C. VM equations

The phase transition criticality condition is

$$R = 6(\dot{H} + H^2) = m^2, \qquad (1)$$

and, defining $M = m^2/(12H_0^2)$, the expansion behavior above and below the phase transition is

$$H^2/H_0^2 = \Omega_m(1+z)^3 + \Omega_r(1+z)^4$$
$$+ M\left\{1 - \left[3\left(\frac{4}{3\Omega_m}\right)^4 M(1-M)^3\right]^{-1}\right\} z > z_t$$
$$(2)$$

$$H^2/H_0^2 = (1-M)(1+z)^4 + M, \qquad z \leq z_t. \qquad (3)$$

The phase transition occurs at

$$z_t = -1 + \frac{3\Omega_m}{4(1-M)} \qquad (4)$$

(for simplicity of the expression we ignore the contribution of radiation energy density Ω_r at $z \lesssim 1$).

We see that above the phase transition, the Universe behaves as one with matter plus a cosmological constant, and after the phase transition it effectively has a dark radiation component (the matter is hidden within this expression) that rapidly redshifts away leaving a de Sitter phase. The original model did not include an explicit high redshift cosmological constant; we see that this implies that

$$\Omega_m = \frac{4}{3}[3M(1-M)^3]^{1/4}. \qquad (5)$$

So there is only one free parameter in the original model, either M or Ω_m, the same number as in ΛCDM. For example, $\Omega_m = 0.3$ implies $M = 0.9017$. We emphasize that the de Sitter behavior at late times is not a result of a cosmological constant, but rather the intrinsic physics of the model.

The effective dark energy equation of state (i.e. of the effective component once the matter contribution has been accounted for) is

$$w(z) = -1 - \frac{1}{3}\frac{3\Omega_m(1+z)^3 - 4(1-M)(1+z)^4}{M + (1-M)(1+z)^4 - \Omega_m(1+z)^3}, \qquad (6)$$

below the phase transition, and simply $w(z > z_t) = -1$ above the phase transition. In the case without a cosmological constant, there is no dark energy above the transition.

The equation of state behavior is phantom, and more deeply phantom as the cosmological constant diminishes, as seen in Fig. 1. Note that for $M > 0.9017$ (in the $\Omega_m = 0.3$ case), the cosmological constant can go negative, and this leads initially to a highly positive equation of state just after the transition. This is not an observationally viable region. As M falls below the critical value, the cosmological constant smooths out the rapid time variation, leading to a nearly constant $w(a)$. If M falls too low, then the transition occurs in the future [see Eq. (4)], and we have simply the ΛCDM model for the entire history to the present. Moreover, M then becomes no longer a free parameter but is given in terms of Ω_m by the requirement that $H(z = 0)/H_0 = 1$. Thus, when considering the elaborated VM model with a free parameter M we put a prior ranging between the lower and upper bounds, corresponding to $z_t \geq 0$ and $\Omega_{de}(z > z_t) \geq 0$, respectively. But again, we regard the original VM model without cosmological constant as the most elegant and theoretically compelling.

III. COSMOLOGICAL PARAMETER FITTING

In order to study the vacuum metamorphosis model we consider a baseline parameter set plus extended scenarios. For our baseline, we consider seven cosmological parameters: the vacuum metamorphosis scale M, and the six parameters of the standard analysis, i.e. the baryon energy

TABLE I. Flat priors on the various cosmological parameters used in this paper. M_{low} and M_{high} are given by conditions described in the text in Eqs. (4) and (5), respectively, as functions of Ω_m.

Parameter	Prior
$\Omega_b h^2$	[0.005, 0.1]
$\Omega_c h^2$	[0.001, 0.99]
τ	[0.01, 0.8]
n_s	[0.8, 1.2]
$\log[10^{10} A_s]$	[2, 4]
Θ_s	[0.5, 10]
M	$[M_{\text{low}}, M_{\text{high}}]$
$\sum m_\nu$ (eV)	[0, 5]
N_{eff}	[0.05, 10]
$\frac{dn_s}{d \ln k}$	[−1, 1]
A_{lens}	[0, 10]
B	[−0.4, 0.4]

density $\Omega_b h^2$, the cold-dark-matter energy density $\Omega_c h^2$, the ratio between the sound horizon and the angular diameter distance at decoupling θ_s, the amplitude and spectral index of the primordial scalar perturbations A_s and n_s (at pivot scale $k_0 = 0.05h$ Mpc^{-1}), and the reionization optical depth τ. All these parameters are varied in a range of external, conservative, priors listed in Table I. For the original VM model, M is fixed by Ω_m (or v.v.) and so there are six parameters, as in ΛCDM.

We also consider two more extended scenarios in addition to our baseline model for testing VM. In the first scenario we add variations in three more parameters: the total neutrino mass for the three standard neutrinos Σm_ν, the running of the scalar spectral index $dn_s/d \ln k$, and the effective number of relativistic degrees of freedom N_{eff}. Finally, in the last scenario, we also consider variation in the gravitational lensing amplitude A_{lens} of the CMB angular power spectra (see e.g. [40]). This scales the CMB lensing strength on all scales by a constant, relative to the prediction of the model being considered.

We analyze these cosmological parameters by making use of the high-ℓ temperature and low-ℓ temperature and polarization CMB angular power spectra released by Planck 2015 [30]. We refer to this data set as "Planck TT," and it includes the large angular-scale temperature and polarization anisotropy measured by the Planck LFI experiment and the small-scale temperature anisotropies measured by Planck HFI. Moreover, we add to Planck TT the high-ℓ polarization data measured by Planck HFI [30], and we refer to this data set simply as "Planck." This is our baseline data. We sometimes also consider the "R16" data set in the form of an external Gaussian prior on the Hubble constant $H_0 = 73.24 \pm 1.74$ km/s/Mpc at 68% C.L., as measured by [2].

In order to derive constraints on the parameters, we use the November 2016 version of the publicly available Monte Carlo Markov chain package `cosmomc` [41]. This code has a convergence diagnostic based on the Gelman and Rubin statistic and includes the support for the Planck data release 2015 Likelihood Code [30] (see [42]), implementing an efficient sampling by using the fast/slow parameter decorrelations [43]. We also consider the impact of CMB foregrounds by including additional nuisance parameters and marginalizing over them as described in [31,44].

IV. VACUUM METAMORPHOSIS COSMOLOGY FITS

A. Original VM

To begin, we consider the original VM model without cosmological constant. This has the same number of dark energy parameters as the standard ΛCDM case, and as we know from Sec. II, it is also consistent with the region in the w_0–w_a phase space preferred by the CMB data. The constraints on cosmological parameters in the case of variation of the standard six parameters are reported in Table II for different choices of data sets. As we can see, assuming VM can indeed raise the Hubble constant but in fact it overshoots the R16 value, with Planck data alone

TABLE II. 68% C.L. constraints on cosmological parameters in the VM scenario for different combinations of data sets.

	Planck TT (VM)	Planck TT +R16 (VM)	Planck (VM)	Planck +R16 (VM)
$\Omega_b h^2$	$0.022\,27^{+0.000\,22}_{-0.000\,25}$	$0.022\,12 \pm 0.000\,22$	$0.022\,25 \pm 0.000\,15$	$0.022\,19 \pm 0.000\,16$
$\Omega_c h^2$	0.1195 ± 0.0021	0.1212 ± 0.0021	0.1198 ± 0.0014	0.1206 ± 0.0015
τ	0.075 ± 0.020	0.068 ± 0.019	0.075 ± 0.018	0.070 ± 0.017
n_s	0.9657 ± 0.0061	0.9616 ± 0.0060	0.9642 ± 0.0047	0.9623 ± 0.0047
$\log(10^{10} A_S)$	3.084 ± 0.037	3.073 ± 0.036	3.085 ± 0.034	3.077 ± 0.032
H_0	78.69 ± 0.56	78.22 ± 0.58	78.61 ± 0.38	78.39 ± 0.39
σ_8	0.930 ± 0.018	0.935 ± 0.017	0.932 ± 0.016	0.933 ± 0.15
S_8	0.814 ± 0.022	0.829 ± 0.022	0.817 ± 0.022	0.823 ± 0.017
$\bar{\chi}^2_{\text{eff}}$	11 279.7	11 287.5	12 964.5	12 972.2

providing a constraint $H_0 = 78.61 \pm 0.38$ (see Table II). This, in practice, replaces one 3σ tension with its opposite.

The VM model and ΛCDM give similar results for most of the parameters, except for H_0 and Ω_m (and σ_8 which depends on Ω_m). This is clearly exhibited in Fig. 3 where we report the two-dimensional posterior distributions from Planck on the six cosmological parameters assuming either VM either a cosmological constant as dark energy

component. The difference in the parameters is mostly associated with the geometric degeneracy in the distance to CMB last scattering.

We also report in Table II the constraints for the VM scenario from the combined Planck + R16 data set. However, as we can notice from the last line of the table, where we report the mean minus log likelihoods, $\bar{\chi}^2_{\text{eff}}$, the inclusion of the R16 prior, that consists in one single data
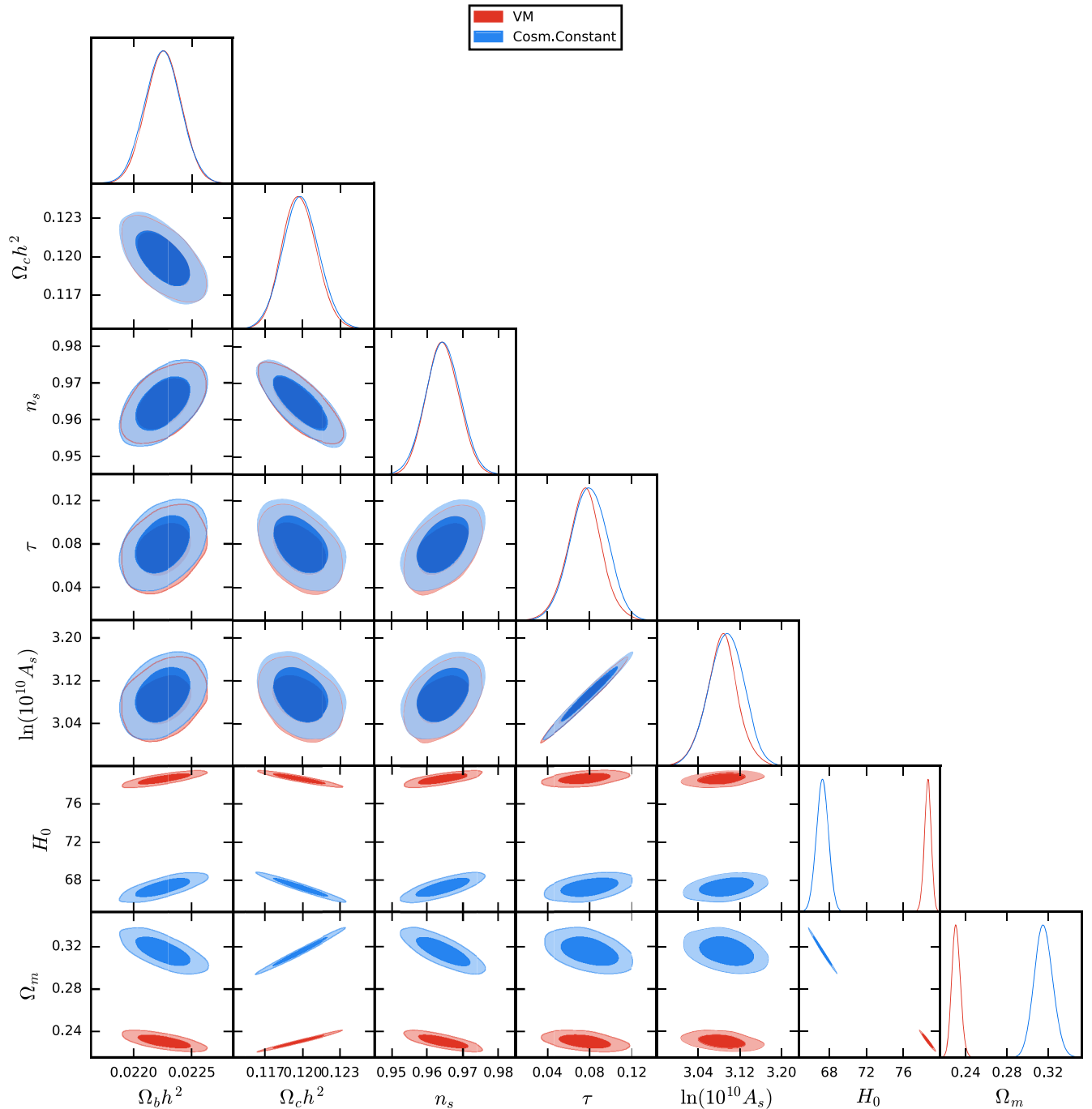

FIG. 3. Triangular plot showing the posteriors of the cosmological parameters for ΛCDM and the original VM model, along with their two-dimensional joint confidence contour at 68% C.L. and 95% C.L. This is for baseline CMB data only, in the six-parameter space.

TABLE III.   68% C.L. constraints on cosmological parameters in the VM scenario, including $\sum m_\nu + N_{\text{eff}} + \frac{dn_s}{d\ln k}$, for different combinations of data sets. For comparison, in the fourth, last, column we report the constraints assuming a cosmological constant for the Planck + R16 data set. If only upper limits are shown, they are at 95% C.L.

	Planck TT +R16 (VM)	Planck (VM)	Planck +R16 (VM)	Planck +R16 (Λ)
$\Omega_b h^2$	$0.021\,97 \pm 0.000\,27$	$0.022\,11 \pm 0.000\,25$	$0.021\,94 \pm 0.000\,20$	$0.022\,57 \pm 0.000\,20$
$\Omega_c h^2$	$0.1146^{+0.0038}_{-0.0043}$	0.1175 ± 0.0034	0.1160 ± 0.0031	0.1223 ± 0.0031
τ	0.080 ± 0.022	0.078 ± 0.020	0.076 ± 0.019	0.093 ± 0.019
n_s	0.941 ± 0.012	0.955 ± 0.012	0.9471 ± 0.0093	0.9778 ± 0.0084
$\log(10^{10}A_S)$	3.081 ± 0.046	3.085 ± 0.041	3.078 ± 0.040	3.127 ± 0.037
H_0	74.0 ± 1.6	$76.5^{+2.3}_{-1.9}$	74.8 ± 1.4	69.7 ± 1.3
$\sum m_\nu$ [eV]	<0.534	<0.503	$0.27^{+0.10}_{-0.25}$	<0.14
N_{eff}	$2.57^{+0.24}_{-0.28}$	2.87 ± 0.23	2.72 ± 0.19	3.31 ± 0.18
$\frac{dn_s}{d\ln k}$	-0.0154 ± 0.0099	-0.0065 ± 0.0079	-0.0091 ± 0.0078	-0.0008 ± 0.0078
σ_8	$0.887^{+0.041}_{-0.029}$	$0.900^{+0.043}_{-0.025}$	$0.877^{+0.039}_{-0.031}$	0.850 ± 0.019
S_8	0.816 ± 0.026	0.809 ± 0.020	0.803 ± 0.022	0.849 ± 0.018
$\bar{\chi}^2_{\text{eff}}$	$11\,281.8$	$12\,966.9$	$12\,968.6$	$12\,976.3$

point, results in an increase of $\Delta\bar{\chi}^2_{\text{eff}} \sim 8$, clearly showing a tension between the Planck data and the R16 prior also in the VM scenario. However, it is worth noticing that while the Planck data set alone in the case of a cosmological constant gives $\bar{\chi}^2_{\text{eff}} = 12967.69$ (see [44]), here we get $\bar{\chi}^2_{\text{eff}} = 12964.64$ for VM, providing a better fit to the same data set with $\Delta\bar{\chi}^2_{\text{eff}} \sim -3$.

When we include in the parameter space the sum of neutrino masses (which must exist), the running of the scalar spectral index, and N_{eff} then VM provides a more consistent picture. The constraints on this nine-parameter VM scenario are reported in Table III for three data combinations (Planck TT, Planck, Planck + R16) and also, for comparison, for the cosmological constant scenario for the Planck + R16 case.

As we can see, in this case we have that the Planck data alone provide the constraint $H_0 = 76.5^{+2.3}_{-1.9}$ at 68% C.L., now in agreement with R16. Moreover, the VM model provides a better mean fit over ΛCDM by $\Delta\bar{\chi}^2_{\text{eff}} = -7.57$ and a value of $H_0 = 74.8 \pm 1.4$ at 68% C.L. for the Planck + R16 case. The shift in H_0 also leads to a lowering of the present dimensionless matter density $\Omega_m = 0.252^{+0.011}_{-0.014}$. The long period of matter domination before the vacuum phase transition enhances growth, and the strongly negative dark energy equation of state means that dark energy density only becomes appreciable at relatively late times. These combine to raise the mass fluctuation amplitude to $\sigma_8 = 0.877^{+0.039}_{-0.031}$ (see Table III). However, note that the weak lensing parameter $S_8 = \sigma_8(\Omega_m/0.3)^{0.5}$ actually decreases relative to the ΛCDM case, from 0.852 ± 0.018 to 0.803 ± 0.022, putting it in better agreement with weak lensing results from the Kilo Degree Survey [45] and Dark Energy Survey [46,47]. Also,

the reduced high redshift $H(z)$ may ameliorate tension in the Lyman alpha-quasar cross-correlations (see [48]).

As we can see from Table III, the agreement with the R16 prior comes at the expense of a smaller value of the neutrino effective number N_{eff} with respect to the standard $N_{\text{eff}} = 3.046$ at the level of $\sim 1.5\sigma$. Also the bounds on neutrino masses are weaker with respect to the cosmological constant case, and some hints are present for a neutrino mass such that $\Sigma m_\nu \sim 0.27$ eV, and for a negative running at the level slightly above 1σ. This should be compared with the same nine-parameter fit under ΛCDM reported in the fourth column of Table III in the case of the Planck + R16 data set. As we can see, the agreement in this case is obtained at the expenses of an higher value for N_{eff} at about 1.5σ, $N_{\text{eff}} = 3.31 \pm 0.18$, and with a strong upper limit on the neutrino mass $\Sigma m_\nu < 0.07$ eV at 68% C.L..

We can, therefore, state that in the case of a nine-parameter analysis both a cosmological constant and VM show some needs for extra physics in order to make the Planck data compatible with the R16 prior. This extra physics is mainly connected with the neutrino effective number N_{eff} that should be larger than the expected value when a cosmological constant is assumed and smaller in the case of VM.

However, as also pointed out in the introduction, the Planck data provides a $\sim 2.5\sigma$ indication for a larger weak lensing CMB spectrum amplitude A_{lens} (see e.g. [49]). While the nature of this anomaly is still unclear, it is clearly interesting to provide constraints also in a further extended scenario, varying also A_{lens}. We report the results of this analysis in Table IV. In this ten-parameter framework, the VM model prefers now a neutrino mass with $\Sigma m_\nu = 0.51 \pm 0.23$ eV at 68% C.L. while the neutrino effective number is perfectly compatible with the standard value

TABLE IV. 68% C.L. constraints on cosmological parameters in the VM scenario, including $\sum m_\nu + N_{\text{eff}} + \frac{dn_s}{d\ln k} + A_{\text{lens}}$, for different combinations of data sets. For comparison, on the fourth, last, column we report the constraints assuming a cosmological constant for the Planck + R16 data set. If only upper limits are shown, they are at 95% C.L.

	Planck TT +R16 (VM)	Planck (VM)	Planck +R16 (VM)	Planck +R16 (Λ)
$\Omega_b h^2$	0.02228 ± 0.00031	0.02231 ± 0.00028	0.02214 ± 0.00022	0.02278 ± 0.00022
$\Omega_c h^2$	$0.1158^{+0.0042}_{-0.0047}$	0.1187 ± 0.0036	0.1172 ± 0.0032	0.1222 ± 0.0031
τ	$0.064^{+0.022}_{-0.025}$	0.059 ± 0.022	$0.058^{+0.021}_{-0.024}$	$0.059^{+0.021}_{-0.021}$
n_s	0.959 ± 0.016	0.966 ± 0.013	0.958 ± 0.011	0.986 ± 0.009
$\log(10^{10} A_S)$	$3.051^{+0.045}_{-0.052}$	3.050 ± 0.044	$3.043^{+0.043}_{-0.049}$	$3.057^{+0.043}_{-0.043}$
H_0	74.6 ± 1.6	76.8 ± 2.3	$74.8^{+1.3}_{-1.4}$	$70.5^{+1.4}_{-1.4}$
$\sum m_\nu$ [eV]	$0.54^{+0.25}_{-0.35}$	<0.829	0.51 ± 0.23	<0.298
N_{eff}	$2.85^{+0.30}_{-0.37}$	3.04 ± 0.26	$2.90^{+0.21}_{-0.24}$	3.41 ± 0.20
$\frac{dn_s}{d\ln k}$	$-0.006^{+0.011}_{-0.013}$	0.0001 ± 0.0088	-0.0021 ± 0.0086	-0.0049 ± 0.0078
A_{lens}	$1.22^{+0.12}_{-0.14}$	$1.17^{+0.09}_{-0.11}$	1.17 ± 0.10	$1.22^{+0.085}_{-0.097}$
σ_8	0.803 ± 0.058	$0.841^{+0.064}_{-0.052}$	$0.811^{+0.047}_{-0.055}$	$0.806^{+0.024}_{-0.033}$
S_8	0.745 ± 0.046	0.761 ± 0.037	0.752 ± 0.035	0.798 ± 0.026
$\bar{\chi}^2_{\text{eff}}$	$11\,280.3$	$12\,965.3$	$12\,966.2$	$12\,971.2$

$N_{\text{eff}} = 3.046$. In the same ten-parameter framework and for the same Planck + R16 data set, but assuming a cosmological constant, we found (see the fourth column in Table IV) that there is no preference for a neutrino mass, with a 68% C.L. upper limit of $\Sigma m_\nu < 0.149$ eV, while we have an indication for $N_{\text{eff}} = 3.41 \pm 0.20$ at 68% C.L., i.e. almost 2σ above the standard value. It is, therefore, clear that in the ten-parameter framework the VM model offers an important advantage over the cosmological constant since it solves the tension on the Hubble constant without the need of a nonstandard value for N_{eff}. In practice, the Planck data under a VM model prefers a value of the Hubble constant larger than the R16 value, but this can be alleviated by introducing a neutrino mass that is well in agreement with current laboratory data (see e.g. [50]). It is also worth noticing that the A_{lens} tension seems somewhat alleviated in the VM scenario and that the value of S_8 is

now in even better agreement with the recent cosmic shear results from the Kilo Degree Survey [45].

We, however, remark that there can be difficulties with other observational data sets not considered here such as redshift space distortions and supernova distances. We leave that for future work. Still, the improvement in χ^2, the defusing of the H_0 tension (and possible amelioration of the weak lensing tension), and of course the strong theoretical foundation of the model together with it having no cosmological constant to explain, makes it worthy of further investigation.

B. Elaborated VM (varying M)

We now consider the more *ad hoc* VM model that includes a cosmological constant; i.e., we allow the vacuum criticality parameter M to float. Constraints are given in Table V considering a scenario based on $6 + 1$

TABLE V. 68% C.L. constraints on cosmological parameters in the elaborated VM scenario, for different combinations of data sets. If only lower limits are shown, they are at 95% C.L..

|	Planck TT	Planck TT +R16	Planck	Planck +R16
$\Omega_b h^2$	0.02224 ± 0.00024	0.02224 ± 0.00023	0.02225 ± 0.00016	0.02224 ± 0.00016
$\Omega_c h^2$	0.1197 ± 0.0022	0.1197 ± 0.0022	0.1199 ± 0.0014	0.1199 ± 0.0014
τ	0.078 ± 0.019	0.077 ± 0.020	0.078 ± 0.017	0.078 ± 0.017
n_s	0.9656 ± 0.0062	0.9657 ± 0.0062	0.9644 ± 0.0048	0.9643 ± 0.0047
$\log(10^{10} A_S)$	3.089 ± 0.037	3.087 ± 0.037	3.092 ± 0.033	3.090 ± 0.033
H_0	$71.5^{+2.8}_{-5.1}$	73.3 ± 1.9	$71.6^{+2.8}_{-5.1}$	73.4 ± 1.8
M	>0.785	$0.889^{+0.022}_{-0.012}$	>0.789	$0.891^{+0.019}_{-0.012}$
σ_8	$0.867^{+0.028}_{-0.048}$	0.883 ± 0.025	$0.870^{+0.028}_{-0.045}$	0.886 ± 0.021
S_8	0.836 ± 0.026	0.831 ± 0.022	0.838 ± 0.022	0.833 ± 0.017
$\bar{\chi}^2_{\text{eff}}$	$11\,281.2$	$11\,282.0$	$12\,966.0$	$12\,966.6$
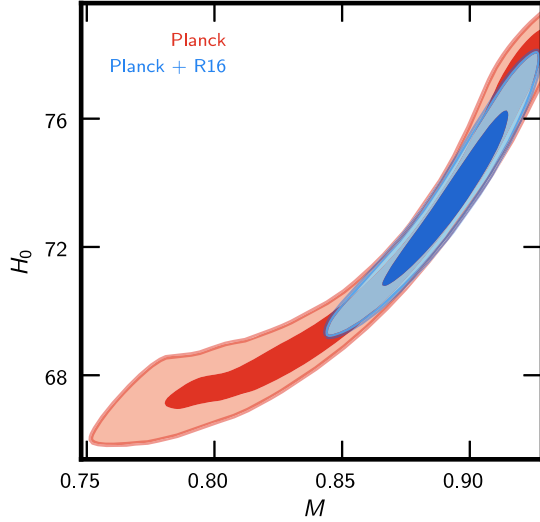
FIG. 4. Constraints on the $M - H_0$ space of the elaborated VM model from the Planck and Planck + R16 data sets in the $6 + 1$ parameters analysis.

cosmological parameters. We can immediately see from the Table that allowing M to float lowers the value of the Hubble constant from the Planck data, making it more compatible with the R16 prior, with $H_0 = 71.5^{+2.8}_{-5.1}$ km/s/Mpc at 68% C.L. Considering the Planck+R16 data set we get $H_0 = 73.4 \pm 1.8$ km/s/Mpc at 68% C.L., with $\Delta\bar{\chi}^2_{\text{eff}} = -5.6$ with respect with the fixed M model reported in Table II, showing that varying M solves the tensions between Planck and R16. This can also be clearly seen in Fig. 4 where we plot the two-dimensional posteriors in the M vs H_0 plane from the Planck and Planck + R16 data sets. Letting M vary allows for lower values of H_0 and the R16 prior is now perfectly compatible with the Planck data. By comparing the $\bar{\chi}^2_{\text{eff}}$ values from the

Planck + R16 data sets for the nine-parameter case in Table III and the ten-parameter case in Table IV, we see that allowing M to float solves the H_0 tension better than the fixed VM or the cosmological constant model, with the inclusion of one extra parameter (in this $6 + 1$ scenario without a neutrino mass parameter).

It is, however, worthwhile to note that the Planck TT and Planck data sets provide only a lower limit to M. Since the maximum theoretical value achievable by M in these runs is given by Eq. (5), corresponding to the fixed M case, this means that the Planck data shows no preference for values of M different from those of the original VM model. This can be also seen by the fact that we have a worse $\bar{\chi}^2_{\text{eff}}$ value when varying M with respect to the fixed case. In practice, the extra parameter space allowed by varying M is not preferred by the Planck data.

In Table VI and Table VII, we report the constraints obtained on cosmological parameters in the case of a varying M model, adding further extra parameters. In Table VI, we include in the analysis also the neutrino effective number N_{eff}, the neutrino mass scale Σm_ν, and the running of the spectral index $\frac{dn_s}{d\ln k}$. As we can see, there is now no indication for values different from the standard expectations for these parameters. In particular, the neutrino effective number N_{eff} is now more compatible with 3.046. But the χ^2 improvement does not exceed the number (one) of extra parameters added to the original VM model, and the elaborated model suffers from the usual cosmological constant problem.

In Table VII, we report similar constraints but now also letting the A_{lens} parameter to vary, for a total variation of 11 parameters. As we can see there is now no indication for extra physics or neutrino mass different from zero as was previously the case for the M fixed model. In practice, there is no need for extra parameters or additional new physics for

TABLE VI. 68% C.L. constraints on cosmological parameters in the elaborated VM scenario, including $\Sigma m_\nu + N_{\text{eff}} + \frac{dn_s}{d\ln k}$, for different combinations of data sets. If only lower limits are shown, they are at 95% C.L.

	Planck TT	Planck TT +R16	Planck	Planck +R16
$\Omega_b h^2$	$0.021\,95^{+0.000\,40}_{-0.000\,46}$	$0.022\,26^{+0.000\,32}_{-0.000\,38}$	$0.022\,06 \pm 0.000\,25$	$0.022\,12^{+0.000\,22}_{-0.000\,25}$
$\Omega_c h^2$	0.1155 ± 0.0054	$0.1183^{+0.0046}_{-0.0053}$	0.1175 ± 0.0033	0.1180 ± 0.0033
τ	0.083 ± 0.023	0.086 ± 0.022	0.082 ± 0.019	0.080 ± 0.019
n_s	0.940 ± 0.024	$0.959^{+0.017}_{-0.021}$	0.953 ± 0.011	0.957 ± 0.011
$\log(10^{10}A_S)$	3.090 ± 0.050	3.104 ± 0.046	3.093 ± 0.039	3.090 ± 0.040
H_0	$66.1^{+5.2}_{-6.4}$	73.0 ± 1.7	$68.6^{+3.9}_{-5.3}$	73.2 ± 1.7
M	>0.742	$0.892^{+0.030}_{-0.008}$	>0.754	$0.899^{+0.020}_{-0.009}$
$\sum m_\nu$ [eV]	<0.640	<0.456	<0.573	<0.428
N_{eff}	$2.61^{+0.42}_{-0.49}$	$2.93^{+0.33}_{-0.43}$	2.84 ± 0.22	2.90 ± 0.21
$\frac{dn_s}{d\ln k}$	-0.016 ± 0.012	-0.009 ± 0.011	-0.0083 ± 0.0081	-0.0064 ± 0.0078
σ_8	0.816 ± 0.057	$0.876^{+0.035}_{-0.028}$	$0.830^{+0.054}_{-0.047}$	$0.875^{+0.024}_{-0.030}$
S_8	0.845 ± 0.031	0.827 ± 0.024	0.836 ± 0.026	0.822 ± 0.022
$\bar{\chi}^2_{\text{eff}}$	$11\,282.8$	$11\,282.8$	$12\,968.6$	$12\,968.0$

TABLE VII. 68% C.L. constraints on cosmological parameters in the elaborated VM scenario, including $\sum m_\nu + N_{\rm eff} + \frac{dn_s}{d\ln k} + A_{\rm lens}$, for different combinations of data sets. If only upper or lower limits are shown, they are at 95% C.L.

	Planck TT	Planck TT +R16	Planck	Planck +R16
$\Omega_b h^2$	$0.022\,87^{+0.000\,56}_{-0.000\,69}$	$0.022\,97^{+0.000\,45}_{-0.000\,39}$	$0.022\,27 \pm 0.000\,28$	$0.022\,39 \pm 0.000\,27$
$\Omega_c h^2$	$0.1214^{+0.0056}_{-0.0071}$	$0.1218^{+0.0050}_{-0.0058}$	0.1188 ± 0.0035	0.1195 ± 0.0034
τ	$0.066^{+0.023}_{-0.026}$	$0.067^{+0.022}_{-0.026}$	0.059 ± 0.021	0.060 ± 0.021
n_s	$0.991^{+0.030}_{-0.035}$	$0.996^{+0.023}_{-0.019}$	0.964 ± 0.013	0.969 ± 0.012
$\log(10^{10}A_S)$	$3.067^{+0.048}_{-0.055}$	$3.070^{+0.047}_{-0.053}$	3.048 ± 0.044	3.052 ± 0.043
H_0	$71.6^{+6.6}_{-7.7}$	73.2 ± 1.7	$67.2^{+3.8}_{-5.4}$	72.9 ± 1.7
M	>0.754	$0.856^{+0.050}_{-0.031}$	>0.724	$0.889^{+0.027}_{-0.010}$
$\sum m_\nu$ [eV]	$0.54^{+0.18}_{-0.50}$	<1.14	$0.51^{+0.20}_{-0.44}$	<0.847
$N_{\rm eff}$	$3.50^{+0.54}_{-0.75}$	$3.57^{+0.43}_{-0.50}$	3.04 ± 0.25	$3.11^{+0.24}_{-0.26}$
$\frac{dn_s}{d\ln k}$	0.005 ± 0.015	$0.007^{+0.012}_{-0.014}$	-0.0005 ± 0.0089	0.0010 ± 0.0082
$A_{\rm lens}$	$1.35^{+0.14}_{-0.17}$	$1.35^{+0.13}_{-0.17}$	$1.22^{+0.10}_{-0.11}$	1.195 ± 0.096
σ_8	$0.748^{+0.080}_{-0.072}$	$0.764^{+0.070}_{-0.054}$	0.745 ± 0.068	$0.807^{+0.051}_{-0.044}$
S_8	0.739 ± 0.051	0.736 ± 0.047	0.772 ± 0.037	0.769 ± 0.037
$\bar{\chi}^2_{\rm eff}$	$11\,279.5$	$11\,279.7$	$12\,965.9$	$12\,966.3$

solving the H_0 tension when varying M. It also important to note that the $A_{\rm lens}$ anomaly is not present in the Planck CMB lensing data derived from trispectrum measurements. The inclusion of the Planck CMB lensing data set could therefore change the results reported in Table VII.

A summary comparing the χ^2 of the VM models with ΛCDM is given in Table VIII.

C. Bayesian evidence

While the χ^2 values reported can give a feeling of the goodness of fit of one model respect to another it is clearly interesting to quantify the better accordance of a model with the data respect to another by using more appropriate statistical methods. This can be done by considering, for example, the marginal likelihood also known as the Bayesian evidence.

Let us remind here some basics of Bayesian parameter inference. Given a vector of parameters $\boldsymbol{\theta}$ of a model M and a set of data $\boldsymbol{x}$, the parameters posterior distribution is given by

$$p(\boldsymbol{\theta}|\boldsymbol{x}, M) = \frac{p(\boldsymbol{x}|\boldsymbol{\theta}, M)\pi(\boldsymbol{\theta}|M)}{p(\boldsymbol{x}|M)} \qquad (7)$$

where $p(\boldsymbol{x}|\boldsymbol{\theta}, M)$ is the likelihood and $\pi(\boldsymbol{\theta}|M)$ is an assumed prior on the parameters.

The marginal likelihood (or evidence) given by

$$E \equiv p(\boldsymbol{x}|M) = \int d\boldsymbol{\theta}\, p(\boldsymbol{x}|\boldsymbol{\theta}, M)\pi(\boldsymbol{\theta}|M), \qquad (8)$$

is a fundamental quantity for Bayesian model comparison. Given two competing models M_0 and M_1 it is indeed useful to consider the ratio of the likelihood probability (the Bayes factor):

$$\ln \mathcal{B} = p(\boldsymbol{x}|M_0)/p(\boldsymbol{x}|M_1) \qquad (9)$$

According to the revised Jeffrey's scale by Kass and Raftery [51], the evidence (against M_1) is considered as "positive" if $\ln \mathcal{B} < -1.0$, "strong" if $\ln \mathcal{B} < -3.0$, and "very strong" if $\ln \mathcal{B} < -5.0$.

In the third column of Table VIII, we report the Bayes factors for several cases, always considering as reference

TABLE VIII. Comparison of the beyond standard physics models with standard ΛCDM. The number of additional parameters relative to ΛCDM is $\Delta N_{\rm par}$, and the improvement in the fit relative to ΛCDM is $\Delta\bar{\chi}^2_{\rm eff}$ In the third column, we provide the bias factor $\ln \mathcal{B}$ computed assuming a cosmological constant as reference model.

Model	$\Delta N_{\rm par}$	$\Delta\bar{\chi}^2_{\rm eff}$	$\ln \mathcal{B}$
Planck only, minimal six parameters:			
ΛCDM	$\cdots$	$\cdots$	0
Vacuum Metamorphosis	0	-3.2	$+1.3$
VM elaborated	1	-1.7	-1.3
Planck only, $+m_\nu$, $N_{\rm eff}$, $\frac{dn_s}{d\ln k}$:			
ΛCDM	$\cdots$	$\cdots$	0
Vacuum Metamorphosis	0	-2.1	0.8
VM elaborated	1	-0.4	-2.2
Planck + R16, $+m_\nu$, $N_{\rm eff}$, $\frac{dn_s}{d\ln k}$:			
ΛCDM	$\cdots$	$\cdots$	0
Vacuum Metamorphosis	0	-7.7	4.9
VM elaborated	1	-8.3	2.0

TABLE IX. 68% C.L. constraints on the amplitude and slope of the scale-dependent scaling of the gravitational lensing amplitude [Eq. (10)], using different data sets.

	Planck TT	Planck TT + lensing	Planck	Planck +lensing
B	Unconstrained	-0.07 ± 0.10	Unconstrained	$-0.076^{+0.11}_{-0.099}$
$A_{\mathrm{lens},0}$	$1.22^{+0.13}_{-0.17}$	$1.014^{+0.068}_{-0.080}$	$1.17^{+0.12}_{-0.15}$	$0.994^{+0.061}_{-0.061}$
$\bar{\chi}^2_{\mathrm{eff}}$	11 276.9	11 293.7	12 963.6	12 979.6

case ($\ln \mathcal{B} = 0$, or M_0 as in the previous definition) the model where the dark energy component is given by a cosmological constant. The evidence is computed from our MCMC chains using the MCEvidence code described in [52,53].

As we can see, when considering the minimal six parameters model we found positive evidence for the vacuum metamorphosis model against a cosmological constant ($\ln \mathcal{B}_{[VM,\Lambda]} = -1.3$). At the same time, we found positive evidence for a cosmological constant against the VM elaborated model despite its better χ^2 value. This can be explained by the extra parameter present in the VM elaborated model since additional parameters are penalized in Bayes comparison.

In extended nine-parameter space, the Planck data alone does not provide a significant evidence for a cosmological constant against a VM model. However, we again found positive evidence against a VM elaborated model both with respect a cosmological constant and the VM model.

Finally, when considering the Planck data set in combination with the R16 value in nine-parameter space, we found a strong evidence for the VM model against a cosmological constant and positive evidence for a VM elaborated model also against a cosmological constant.

V. SCALE-DEPENDENT LENSING AMPLITUDE

In a second approach to beyond standard physics, we test the "Planck" data set with a scale-dependent scaling of the gravitational lensing amplitude. This seeks to explore indications that cosmological parameters derived from the lower multipole ($\ell \lesssim 1000$) data and the higher multipole ($\ell \gtrsim 1000$) data can differ by $\sim 1\sigma$. In this case, in addition to the six parameters of the standard ΛCDM model (VM is not used in this section), we reparametrize A_{lens} from a constant (seventh parameter) to both an amplitude and a slope, giving eight parameters in total.

Specifically,

$$A_{\mathrm{lens}} = A_{\mathrm{lens},0} \times \left[1 + B \log_{10} \left(\frac{\ell}{300} \right) \right]. \qquad (10)$$

This form is motivated by the behavior of various beyond standard scale-dependent physics, such as modified gravity, neutrino mass, and cold dark energy, investigated in [54]. The amplitude $A_{\mathrm{lens},0}$ is the value at $\ell = 300$, in the vicinity

of the first acoustic peak, and roughly represents the mean over the full multipole range.

The constraints on $A_{\mathrm{lens},0}$ and B are reported in Table IX for several combinations of data sets. The Planck TT and Planck data sets both favor a value for $A_{\mathrm{lens},0}$ larger than the expected value, while the B parameter is unconstrained. Comparing to the standard ΛCDM case, the parameter values do not shift appreciably and the χ^2 improves by less than 0.4 (at the cost of 1 more parameter). However, we found that these mild shifts are in the right direction to alleviate the several tensions. We found that for the Planck data set the Hubble constant is now constrained to be $H_0 = 67.86 \pm 0.74$ km/s/Mpc at 68% C.L., i.e. bringing the tension with the R16 prior from 3.24 standard deviations to 2.87. Also the S_8 parameter is smaller and now constrained from the Planck data set to be $S_8 = 0.818 \pm 0.024$ at 68% C.L., in better agreement with cosmic shear measurements.

The one additional parameter B cannot be determined with the "Planck" data set alone. To constrain the scale dependence of the lensing amplitude, we must include CMB lensing data, i.e. use the lensing potential power spectrum derived from the CMB trispectrum analysis; we refer to this as "Planck + lensing." Table IX summarizes the results, and Fig. 5 shows the one-dimensional and joint probability distributions of the lensing amplitude parameters.

The positive correlation between $A_{\mathrm{lens},0}$ and B can be understood as preserving the CMB lensing power spectrum amplitude where it has the most power, at $\ell < 300$.

The inclusion of the lensing data brings the value of $A_{\mathrm{lens},0}$ back in agreement with the standard value, and it now constrains the slope to be $B = -0.076^{+0.11}_{-0.099}$. We find negligible shift in the cosmological parameters. Thus, this form of scale dependence (linear in $\log \ell$) cannot solve the H_0 tension.[1]

We remark, however, by looking at the last line in Table IX, that the inclusion of CMB lensing to the Planck data set significantly increases the $\bar{\chi}^2_{\mathrm{eff}}$ by ~ 16. Since the CMB lensing consists of about eight data points, this clearly shows a significant tension between the Planck and

---

[1]Note that the scale-dependent physics considered in [54] does lead to a negative value of $B \approx -0.015$ for the massive neutrino and cold dark energy cases (while B has a positive sign for the $f(R)$ gravity case). Current experimental precision is insufficient to constrain such scale-dependent physics.
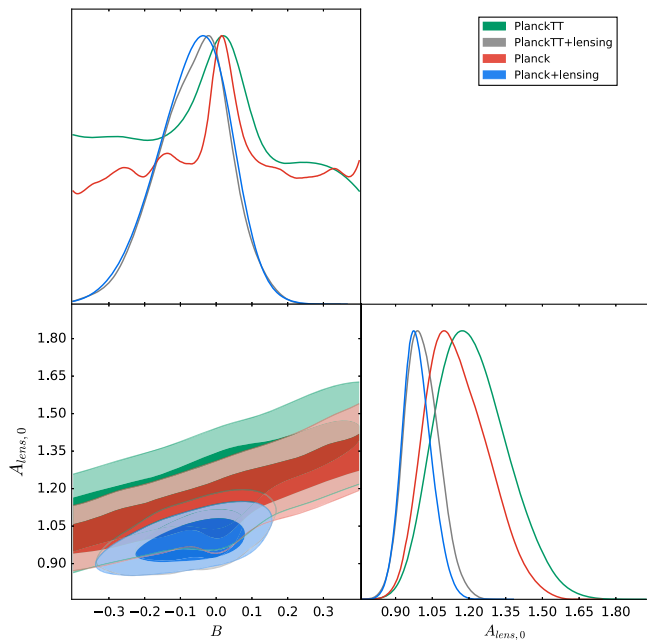
FIG. 5. Triangular plot showing the posteriors of $A_{\mathrm{lens,0}}$ and B for the data sets considered, as well as their two-dimensional joint confidence contour at 68% C.L.

lensing data sets that not even a scale dependence for A_{lens} seems able to solve.

VI. CONCLUSIONS

Current CMB and local Hubble constant data, taken at face value and interpreted within a ΛCDM cosmological model, show a tension in the value of H_0. This tension can be removed by taking the dark energy not to be near cosmological constant behavior but with a very unusual nature—deeply phantom and rapidly evolving. Rather than treating this phenomenologically, we resuscitate the vacuum metamorphosis theory of Parker and collaborators, involving a phase transition in the nature of gravity and the vacuum, based on calculations within quantum gravity.

We demonstrate that vacuum metamorphosis provides a solution to the H_0 tension, and indeed yields an improvement in χ^2 by 7.5 over ΛCDM with the same number of parameters. Moreover, it can also ameliorate possible tension in the weak lensing amplitude S_8 seen between

Planck and some ground based surveys. Given the theory's robust foundation and reasonable motivation, including no explicit or implicit cosmological constant, it is worthwhile to investigate it further in future work, in particular examining consistency with further data sets such as baryon acoustic oscillations and supernova distances.

Considering Bayesian evidence, we found, for the Planck data set alone, positive evidence for a VM model against a cosmological constant both in the six- and nine-parameter framework. When the R16 data set is considered, we found a strong evidence for the VM model against a cosmological constant in nine-parameter space.

Another extension of the standard model involves scale dependence of the CMB lensing amplitude A_{lens}, beyond what exists in the standard model. This has a more modest motivation, from the lesser apparent tension between cosmological parameters derived from CMB data at high and low multipoles (roughly less than and greater than $\ell \approx 1000$). Such scale dependence could arise from beyond standard model physics such as modified gravity, cold dark energy, or massive neutrinos. We do not find any evidence for a tilt in the CMB lensing amplitude, though the Planck lensing data is not precise enough to constrain this tightly.

Future CMB data from stage 3 experiments, and particularly from a CMB stage 4 experiment, can continue to test the nature of dark energy, beyond standard physics, and consistency between the high and low redshift universe. Any solution must fit the rich array of data. All together will evaluate tensions and anomalies and shed light on whether we are seeing systematics, statistical excursions, or indeed new physics, perhaps even definite signs of quantum gravity.

ACKNOWLEDGMENTS

[1] W. L. Freedman, B. F. Madore, V. Scowcroft, C. Burns, A. Monson, S. E. Persson, M. Seibert, and J. Rigby, Astrophys. J. **758,** 24 (2012).

[2] A. G. Riess *et al.*, Astrophys. J. **826,** 56 (2016).

[3] Q. G. Huang and K. Wang, Eur. Phys. J. C **76,** 506 (2016).

[4] J. L. Bernal, L. Verde, and A. G. Riess, J. Cosmol. Astropart. Phys. 10 (2016) 019.

[5] T. Karwal and M. Kamionkowski, Phys. Rev. D **94,** 103523 (2016).

[6] P. Ko and Y. Tang, Phys. Lett. B **762,** 462 (2016).

[7] S. Kumar and R. C. Nunes, Phys. Rev. D **94,** 123511 (2016).

[8] S. Joudaki *et al.*, Mon. Not. R. Astron. Soc. **471,** 1259 (2017).

[9] A. Shafieloo, D. K. Hazra, V. Sahni, and A. A. Starobinsky, Mon. Not. R. Astron. Soc. **473,** 2760 (2018).

[10] B. Santos, A. A. Coley, N. C. Devi, and J. S. Alcaniz, J. Cosmol. Astropart. Phys. 02 (2017) 047.

[11] V. Prilepina and Y. Tsai, J. High Energy Phys. 09 (2017) 033.

[12] G. B. Zhao *et al.*, Nat. Astron. **1,** 627 (2017).

[13] M. M. Zhao, D. Z. He, J. F. Zhang, and X. Zhang, Phys. Rev. D **96,** 043520 (2017).

[14] W. Yang, R. C. Nunes, S. Pan, and D. F. Mota, Phys. Rev. D **95,** 103522 (2017).

[15] Y. Zhang, H. Zhang, D. Wang, Y. Qi, Y. Wang, and G. B. Zhao, Res. Astron. Astrophys. **17,** 050 (2017).

[16] C. Brust, Y. Cui, and K. Sigurdson, J. Cosmol. Astropart. Phys. 08 (2017) 020.

[17] J. Solà, A. Gómez-Valent, and J. de Cruz Pérez, Int. J. Mod. Phys. A **32,** 1730014 (2017).

[18] B. Follin and L. Knox, arXiv:1707.01175.

[19] S. M. Feeney, D. J. Mortlock, and N. Dalmasso, arXiv:1707.00007.

[20] B. R. Zhang, M. J. Childress, T. M. Davis, N. V. Karpenka, C. Lidman, B. P. Schmidt, and M. Smith, Mon. Not. R. Astron. Soc. **471,** 2254 (2017).

[21] S. Dhawan, S. W. Jha, and B. Leibundgut, Astron. Astrophys. **609,** A72 (2018).

[22] E. Di Valentino, A. Melchiorri, E. V. Linder, and J. Silk, Phys. Rev. D **96,** 023523 (2017).

[23] L. Parker and A. Raval, Phys. Rev. D **62,** 083503 (2000).

[24] L. Parker and D. A. T. Vanzella, Phys. Rev. D **69,** 104009 (2004).

[25] R. R. Caldwell, W. Komp, L. Parker, and D. A. T. Vanzella, Phys. Rev. D **73,** 023513 (2006).

[26] G. E. Addison, Y. Huang, D. J. Watts, C. L. Bennett, M. Halpern, G. Hinshaw, and J. L. Weiland, Astrophys. J. **818,** 132 (2016).

[27] Planck Collaboration, Astron. Astrophys. **607,** A95 (2017).

[28] J. W. Henning *et al.*, Astrophys. J. **852,** 97 (2018).

[29] K. Aylor *et al.*, Astrophys. J. **850,** 101 (2017).

[30] N. Aghanim *et al.* (Planck Collaboration), Astron. Astrophys. **594,** A11 (2016).

[31] E. Di Valentino, A. Melchiorri, and J. Silk, Phys. Lett. B **761,** 242 (2016).

[32] M. Betoule *et al.* (SDSS Collaboration), Astron. Astrophys. **568,** A22 (2014).

[33] F. Beutler, C. Blake, M. Colless, D. Heath Jones, L. Staveley-Smith, L. Campbell, Q. Parker, W. Saunders, and F. Watson, Mon. Not. R. Astron. Soc. **416,** 3017 (2011).

[34] A. J. Ross, L. Samushia, C. Howlett, W. J. Percival, A. Burden, and M. Manera, Mon. Not. R. Astron. Soc. **449,** 835 (2015).

[35] L. Anderson *et al.* (BOSS Collaboration), Mon. Not. R. Astron. Soc. **441,** 24 (2014).

[36] A. A. Starobinsky, Phys. Lett. B **91,** 99 (1980).

[37] A. Sakharov, Sov. Phys. Dokl. **12,** 1040 (1968); Gen. Relativ. Gravit. **32,** 365 (2000).

[38] E. V. Linder, Phys. Rev. Lett. **90,** 091301 (2003).

[39] R. de Putter and E. V. Linder, J. Cosmol. Astropart. Phys. 10 (2008) 042.

[40] E. Calabrese, A. Slosar, A. Melchiorri, G. F. Smoot, and O. Zahn, Phys. Rev. D **77,** 123531 (2008).

[41] A. Lewis and S. Bridle, Phys. Rev. D **66,** 103511 (2002).

[42] A. Lewis and S. Bridle, http://cosmologist.info/cosmomc/.

[43] A. Lewis, Phys. Rev. D **87,** 103529 (2013).

[44] P. A. R. Ade *et al.* (Planck Collaboration), Astron. Astrophys. **594,** A13 (2016).

[45] F. Köhlinger *et al.*, Mon. Not. R. Astron. Soc. **471,** 4412 (2017).

[46] DES Collaboration, arXiv:1708.01530.

[47] M. A. Troxel *et al.*, arXiv:1708.01538.

[48] H. du Mas du Bourboux *et al.*, arXiv:1708.02225.

[49] N. Aghanim *et al.* (Planck Collaboration), Astron. Astrophys. **596,** A107 (2016).

[50] F. Capozzi, E. Di Valentino, E. Lisi, A. Marrone, A. Melchiorri, and A. Palazzo, Phys. Rev. D **95,** 096014 (2017).

[51] R. E. Kass and A. Raftery, J. Am. Stat. Assoc. **90,** 773 (1995).

[52] A. F. Heavens, Y. Fantaye, A. Mootoovaloo, H. Eggers, Z. Hosenie, S. Kroon, and E. Sellentin, Phys. Rev. D **93,** 023528 (2016).

[53] A. Heavens, Y. Fantaye, E. Sellentin, H. Eggers, Z. Hosenie, S. Kroon, and A. Mootoovaloo, Phys. Rev. Lett. **119,** 101301 (2017).

[54] A. Hojjati and E. V. Linder, Phys. Rev. D **93,** 023528 (2016).